TECHNIQUE FOR THE EVALUATION OF EARTHQUAKE-INDUCED LATERAL SPREADING

Michael K. Sharp[1] and Ricardo Dobry[2]
[1]Waterways Experiment Station, [2]Rensselaer Polytechnic Institute

ABSTRACT

The current state of the practice for evaluating liquefaction triggering is to calculate the cyclic stress ratio and the cyclic resistance ratio from correlations with either the standard penetration, cone penetration, shear wave, or Becker penetration field tests. Determination of the amount of lateral spreading that occurs is based on empirical correlations with observed field data. This paper reports the results of a research study to investigate the effect of permanent lateral ground displacements due to seismically induced liquefaction and lateral spreading, and to correlate both liquefaction triggering and lateral spreading with field data, namely the cone penetrometer test. This research involved centrifuge testing utilizing a miniature cone penetrometer system suitable for testing in-flight.

INTRODUCTION

Liquefaction of loose, water-saturated sands and other granular soils due to earthquake shaking is a major cause of damage to and destruction of constructed facilities. One of the major liquefaction induced types of ground failure is lateral spreading of mildly sloping ground. A 2-year research effort focusing on evaluation of permanent lateral ground deformation (D_H) due to lateral spreading using the in situ static cone penetration testing (CPT) technique has been conducted at Rensselaer Polytechnic Institute (RPI), Troy, NY. In this investigation, lateral spreading D_H measurements are directly correlated with the CPT in centrifuge model tests for various sand relative densities and degrees of pre-shaking. These correlations, after proper verification against the available empirical and case history information related to both CPT and D_H in the field provide the basis for CPT-based charts to predict D_H in the field for given ground slope, soil conditions, and strong motion input. Also, these charts provide further clarification of the threshold combinations of CPT value, soil depth, ground slope, and strong motion input for which D_H becomes small and can be neglected even if the soil liquefies, due to its dilatant shear stress-strain response.

This research employs physical prototype modeling using the centrifuge facilities at RPI and the development of a miniature CPT and containers appropriate for centrifuge testing. Several investigators have also shown promising results of modeling the CPT in sand in the centrifuge, with results reported by Phillips and Valsangkar (1987), Corte et al. (1991), and Renzi et al. (1994). The results reported by Corte, and Renzi have also shown that a CPT profile conducted in the centrifuge can be used to predict tip resistance, q_c, in the field. Extensive work at RPI using a laminar box container inclined to the horizontal and shaken at the base have demonstrated the usefulness of centrifuge simulation of the lateral spreading phenomenon (Dobry et al., 1995; Taboada, 1995).

DEVELOPMENT OF MINIATURE CPT SYSTEM

The system consists of a miniature CPT appropriate for testing in the centrifuge, with three miniature cones used in conjunction with the soil model container. The in-flight CPT

(Fig. 1) is an electric chain driven system capable of penetrating into the soil model a distance of 1 m. The soil model container is cylindrical with a diameter of 50 cm and height in excess of 1 m. It is possible to model a soil deposit with a maximum field thickness of approximately 20 m. The miniature cones have diameters of 4, 8, and 12 mm, respectively. The use of three different cones was planned such that varying centrifugal accelerations could be tested while still maintaining the proper scaling relationship with the standard field CPT. That is, the 4 mm cone is being used at a centrifuge acceleration of 9g, the 8 mm cone at 4.5g, and the 12 mm cone at 3g, with all of them modeling the prototype CPT in the field at 1g having the standard diameter of 36 mm. In this way, each one of the cones serves as a 'model of the models' for the others, thus increasing the confidence of the results.

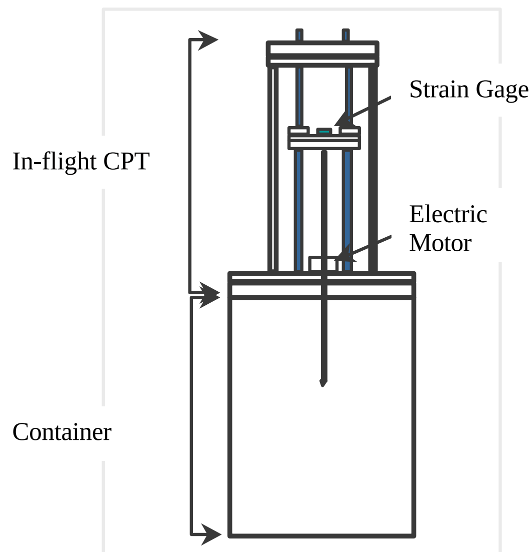

Figure 1. Schematic of In-flight CPT

Container size and boundary conditions can affect CPT measurements. Several researchers (Parkin and Lunne, 1982, Renzi et al., 1994) have investigated the influence of boundary conditions on CPT data and have established a diameter ratio, R_d, defined as the ratio of the chamber diameter to cone diameter. These results indicate that the side boundary effects depend on the relative density of the sand. For loose sand with relative density on the order of 30%, the side boundary effects are negligible. For dense sand the chamber diameter must be at least 50 times the diameter of the cone to eliminate the effect of the side boundary on cone resistance. The results of work in a rigid walled chamber report diameter ratios of 28 to 39.7. These results indicate that for rigid walled chambers the side boundary effects are not significant when the diameter ratio is greater than 28. For the penetrometers and container developed at the RPI centrifuge, the minimum R_d values for the 4, 8 and 12 mm cones for pushes located at the center of the container are 125, 62.5, and 41.6 respectively. These values are larger than those reported in the literature and should assure that no boundary effects will occur for pushes made at the center of the container. In addition to the center of the container, pushes are also performed in the RPI investigation along two concentric circles, with the outer circle being 10 cm from the container's edge. Pushes made close to the boundary would allow the failure mechanism to develop freely on the side of the probe away from the boundary but will be constrained on the side toward the boundary. In this case side-wall boundary effects are negligible even when the probe is located at a distance from the wall corresponding to $R_d = 5$. Using 10 cm as the distance to the wall gives R_d values of 25, 12.5, and 8.3 for the three cones used at RPI. As shown later by the preliminary results of in-flight cone penetration at RPI, these cone diameters and push locations showed no effect from the side-wall boundaries, as expected.

With respect to the bottom boundary effect, Phillips and Valsangkar (1987) reported that for a 10 mm cone, the bottom boundary effects are seen starting at a vertical distance of 10 to 12 cone diameters. In the case of the cones used in this experiment, the expected distance of bottom influence would be 48 mm for the 4 mm cone, 96 mm for the 8 mm cone, and 144 mm for the 12 mm cone. The tests at RPI reveal a bottom influence at vertical distances from the bottom consistent with these and others reported in the literature.

The prototype standard penetration rate for the CPT in the field is 2 cm/sec; for the in-flight tests being conducted at the RPI centrifuge the model penetration rate is 1 mm/sec. Phillips and Valsangkar (1987), and Corte et al., (1991) reported results of centrifuge tests in sand performed at penetration rates of 0.5-10 mm/sec with no noticeable difference in results. The penetration test appears to be a drained event in saturated sand. The rate of 1 mm/sec for the tests being conducted at RPI is believed to be consistent with prototype measurements, and also to be slow enough so as to assure drained conditions when a saturated sand model is tested.

The soil selected for these experiments is Nevada sand, having geotechnical properties as previously measured by Arulmoli et al. (1992). This is the same sand that will be used for the lateral spreading experiments in the laminar box. The specific gravity of Nevada sand was determined to be 2.67 and the maximum and minimum densities were found to be 17.33 kN/m^3 (minimum void ratio = 0.511) and 13.87 kN/m^3 (maximum void ratio = 0.887), respectively. The grain size ranges from 0.1 to 0.25 mm and the soil classifies as a fine sand. Renzi et al., (1994) reported that soil particle size does not affect the results for a ratio d_c / d_{50} in the range of 90 to
50, where d_c is the model cone diameter. For Nevada sand, d_{50} = 0.13 mm, which gives d_{4mm} / d_{50} = 30.7, d_{8mm} / d_{50} = 61.5, and d_{12mm} / d_{50} = 92. No grain size effects were observed in the data for the RPI cones, as indicated by the excellent 'model-of-the-model' comparisons with the other cones.

CPT CENTRIFUGE TESTS PERFORMED AND RESULTS

Centrifuge results reported in this paper are from in-flight CPT on several relative densities and dry and saturated Nevada sand models. The sand was placed dry using the sand raining technique. In-flight CPT tests were performed on five models with nine to twelve cone penetrometer probes per model. A typical model was tested with each of the three probes (4, 8, and 12 mm) and three to four tests per probe. The tests were conducted by starting at the lowest g level, 12 mm at 3g, and finishing at the highest g level, 4 mm at 9g. The models tested were as follows; D_r=75% dry, D_r=75% saturated, D_r=65% dry, D_r=45% dry and D_r=45% saturated. A typical set of results is shown in Fig. 2. The agreement is excellent, confirming the 'model of the models' concept, as well as the agreement between dry versus saturated models at the same effective vertical stress, σ'_{vo}. This agreement of q_c versus σ'_{vo} for dry versus saturated data, allows us to assume a fully submerged deposit to a depth of about 20 m, despite the fact that the q_c measurements in the fully saturated sand models reached only to about 10 m prototype. Utilizing the plots for the data collected from the three different relative densities (75%, 65%, and 45%), and correcting the data for overburden pressure allows the creation of a plot as shown in Fig. 3. The parameter q_{c1} depends on the relative density of the soil and from the in-flight CPT tests of this experiment, the values are as shown in Fig. 3. These values and trends with σ'_{vo} are in excellent agreement with those reported by Olsen (1994) and others. Also shown in Fig. 3 are the results of CPT data collected in models that were either overconsolidated or pre-shaken. Notice that the model with an OCR = 4 and the pre-shaken model (both deposited to a D_r = 45%) have CPT values in line with the D_r = 75% models. The significance of this is that CPT data collected in the field would incorporate the effects of overconsolidation and prior history of the deposit.

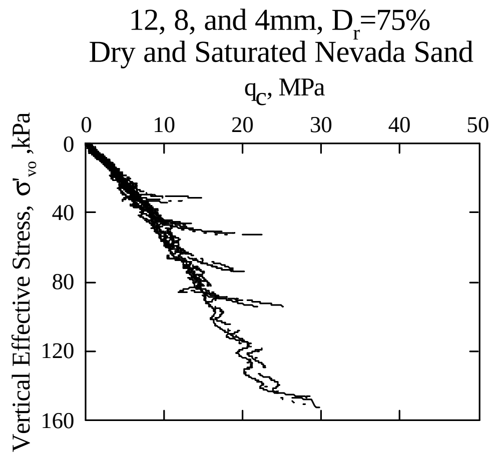

Figure 2. Results from D_r = 75% tests, dry and Saturated sand

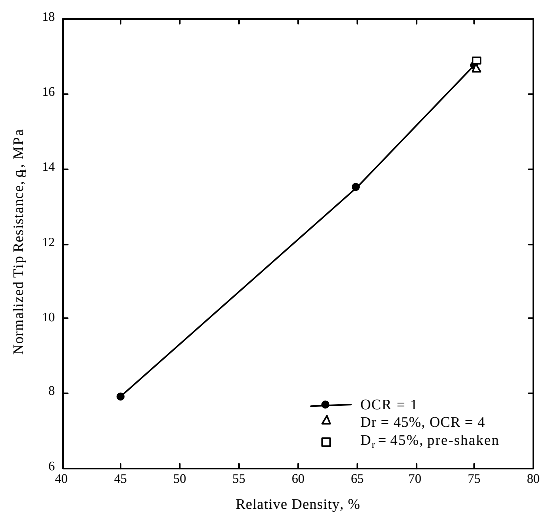

Figure 3. Relative density versus q_{c1} from CPT tests

LIQUEFACTION INDUCED LATERAL SPREADING TESTS PERFORMED AND RESULTS

A total of eleven tests were conducted to examine the effects of relative density, peak acceleration, thickness of deposit, overconsolidation, and pre-shaking on both the thickness of liquefied layer and the amount of lateral spreading induced by liquefaction of a uniform deposit simulating a gentle, infinite slope. The models were constructed to the same relative densities as those used for the CPT models (45%, 65%, and 75%) and saturated. Peak accelerations were either 0.2 or 0.4g, thickness of deposit was either 6 or 10 m, and overconsolidated models had an OCR = 4. Figure 4 shows the inclined RPI laminar box container and typical model with instrumentation used to model lateral spreading in the centrifuge. The model is excited in-flight at the base of the container by a simulated earthquake acceleration time history. This earthquake excitation causes the soil to liquefy, and downslope permanent lateral displacements develop in the liquefied soil by the combined effect of static and dynamic shear stresses. Acceleration, pore pressure, and vertical and horizontal displacements measure the corresponding parameters during and after shaking. Accelerometers and pore pressure transducers in the model allow for the determination of the thickness of liquefied layer. Vertical displacement transformers measure the amount of settlement and horizontal displacement transformers measure the lateral spread and permit determination of shear strains in the deposit.

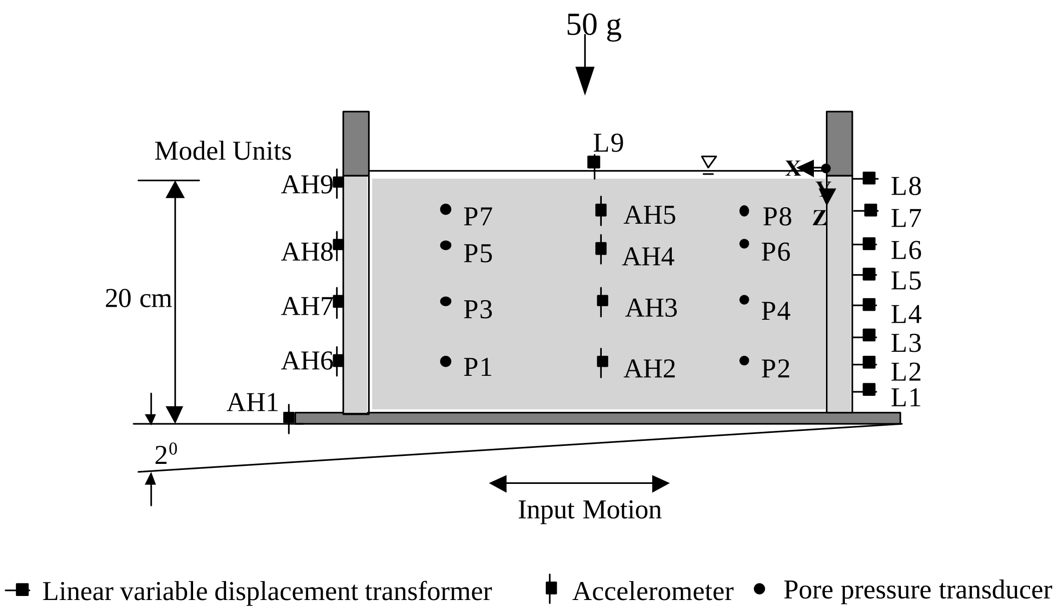

Figure 4. RPI laminar box and model setup for liquefaction tests

From the tests conducted a plot such as shown in Fig. 5 can be constructed which plots relative density versus amount of lateral spread. A similar plot can be made for D_r versus thickness of liquefied layer or D_r versus settlement. Notice that the plot incorporates the 6 and 10 m thick deposit data, the varying peak acceleration, effects of overconsolidation, and pre-shaking.

The data shown in the plot for the 6 m thick deposit represents work done to investigate the effects of overconsolidation and pre-shaking. Tests were conducted on models constructed at relative densities of 45% and 75%. Two Dr = 45% models were constructed, one tested at an OCR equal to one and a second at an OCR equal to four. The D_r = 75% model was constructed and tested at an OCR equal to one. Increasing the g level to four times the normal testing level, holding the model at this level for several minutes and then decreasing the g level to normal testing range overconsolidated the model. Similar tests were conducted with models tested with the cone penetrometer, to determine the effects of overconsolidation on both liquefaction and tip resistance. Notice in Fig. 5 that the models constructed to a relative density of 45% and 75% with an OCR=1 are behaving in a manner similar to the results from the 10 m thick deposits. Increasing relative density produces a corresponding decrease in amount of liquefaction and lateral spreading. However, it is shown in Fig. 5, that the model constructed to a D_r = 45% and tested at an OCR=4 is behaving very much like the model at D_r =75% and OCR=1. There is also a corresponding increase in the tip resistance from the OCR=1 to OCR=4 models although both were constructed to D_r = 45%. This would led to the conclusion, based on limited testing, that the effects of overconsolidation can be detected by the cone penetrometer and correctly predict the liquefaction effects.

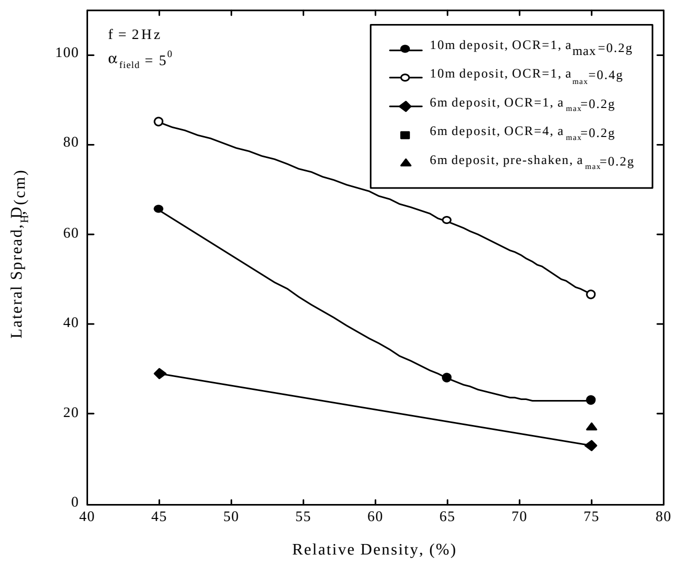

Figure 5. Relative density versus lateral spread

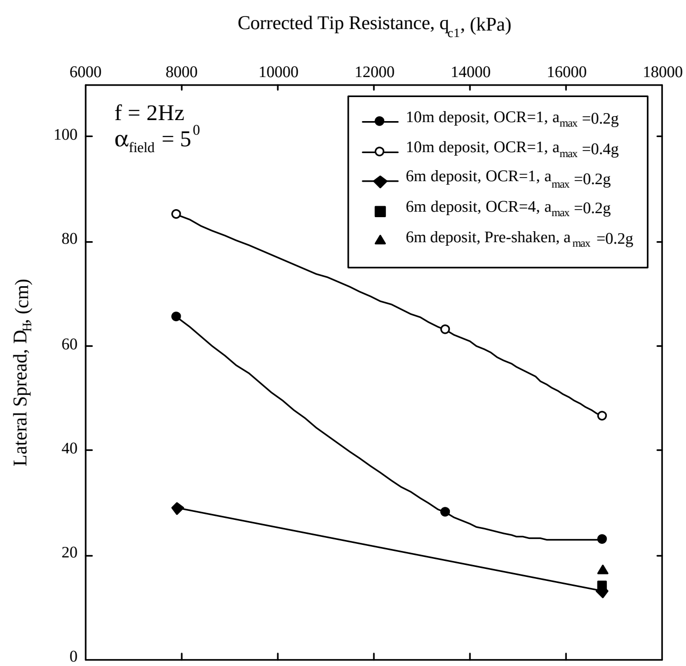

Figure 6. Corrected tip resistance versus lateral spread for 10 and 6 m thick deposits

Also shown in Fig. 5 are the results of the pre-shaking tests. Two models were constructed to D_r = 45%, one tested with no pre-shaking and one subsequent to pre-shaking. The pre-shaking was done on dry models before saturation and with very few cycles of shaking such that the change in relative density was less than 5%. Similar tests were conducted with the cone penetrometer also to determine the effects on tip resistance. The data is seen to plot very closely to the D_r = 75%, OCR = 1 and the D_r = 45%, OCR = 4 results. This would led to the conclusion that the cone penetrometer is capable of responding to the effects produced in the soil by its prior history. This is based on a limited number of tests and more work needs to be performed in this area.

By combining the results shown in Fig. 3 with those shown in Fig. 5, a plot of corrected tip resistance versus lateral spread (or alternatively thickness of liquefied layer or settlement) can be made and shown in Fig. 6. This plot then is a prediction chart for determining the amount of lateral displacement based on the corrected tip resistance field data. However, the plot is for a specific type of deposit and level of shaking. The data represents a deposit of clean sand either 6 or 10 m thick with a 5^0 slope, shaken with a peak acceleration of 0.2 or 0.4 g at a frequency of 2 Hz. Current work is focusing on generalizing these results to include variables such as different deposits, varying permeability, and varying earthquake shaking.

CONCLUSION

This paper has presented results from research aimed at improving the evaluation of earthquake-induced liquefaction and subsequent results such as lateral spreading. By incorporating results from centrifuge cone penetration testing and laminar box liquefaction testing, a methodology for the development of prediction charts has been established. Work is continuing to enhance these charts to incorporate more variables such as different deposit thickness, varying permeability, and varying earthquake shaking. This research also presented promising results concerning the effects of overconsolidation and pre-shaking and the ability of the cone penetrometer to correctly incorporate these effects into the prediction of liquefaction. More testing needs to be done in this area to substantiate and verify the results presented herein.

REFERENCES

Arumoli, K., K.K. Muraleetharan, M.M. Hossain and L.S. Fruth (1992), "Verification of Liquefaction Analysis by Centrifuge Studies Laboratory Testing Program Soil Data Report," Report from The Earth Technology Corporation, Irvine, California.

Corte, J.F., J. Garnier, L.M. Cottineau & G. Rault, (1991). "Determination of Model Soil Properties in the Centrifuge," Proc. of Int. Conf. Centrifuge 1991, Boulder, CO, 13-14 June, pp. 607-614.

Dobry, R., V. Taboada, and L. Liu (1995). "Centrifuge modeling of liquefaction effects during earthquakes," Proc. First Intl. Conf. on Earthquake Geotechnical Engineering, Tokyo, Japan, November, Vol. 3.

Olsen, R.S. (1994). "Normalization and Prediction of Geotechnical Properties Using the Cone Penetrometer Test (CPT)", Technical Report GL-94-29, U.S. Army Waterways Experiment Station.

Parkin, A. K. and Lunne, T. (1982). "Boundary Effects in the Laboratory Calibration of a Cone Penetrometer in Sand," Proceedings of the Second European symposium on Penetration Testing, ESOPT II, Amsterdam, May 1982. Vol. 2, pp. 761-768.

Phillips, R. and A. J. Valsangkar, (1987). “An Experimental Investigation of Factors Affecting Penetration Resistance in Granular Soils in Centrifuge Modeling,” Report CUED/D-Soils TR 210, Cambridge.

Renzi, R., J.F. Corte, G. Bagge, M. Gui, J. Laue, (1994). “Cone Penetration Tests in the Centrifuge: Experience of Five Laboratories,” Proc. of International Conference Centrifuge 94, Singapore, 31 August-2 September, pp. 77-82.

Taboada, V.M. (1995). “Centrifuge Modeling of Earthquake-Induced Lateral Spreading in Sand Using a Laminar Box”, PhD Thesis, Rensselaer Polytechnic Institute, Troy, NY.